JOURNAL OF VIROLOGY, Nov. 1996, p. 8071–8080 Vol. 70, No. 11
0022-538X/96/$04.00+0

Transduction of *Notch2* in Feline Leukemia Virus-Induced Thymic Lymphoma

JENNIFER L. ROHN,[1] ADAM S. LAURING,[1] MICHAEL L. LINENBERGER,[2] AND JULIE OVERBAUGH[1]*

Department of Microbiology[1] and Division of Hematology, Department of Medicine,[2] University of Washington, Seattle, Washington 98195

Received 2 April 1996/Accepted 25 July 1996

Feline leukemia virus (FeLV) is thought to induce neoplastic diseases in infected cats by a variety of mechanisms, including the transduction of host proto-oncogenes. While FeLV recombinants that encode cellular sequences have been isolated from tumors of naturally infected animals, the acquisition of an unrelated host gene has never been documented in an experimental FeLV infection. We isolated recombinant FeLV proviruses encoding feline *Notch2* sequences from thymic lymphoma DNA of two cats inoculated with the molecularly cloned virus FeLV-61E. Four recombinant genomes were identified, three in one cat and one in the other. Each had similar but distinct transduction junctions, and in all cases, the insertions replaced most of the envelope gene with a region of *Notch2* that included the intracellular ankyrin repeat functional domain. The product of the FeLV/*Notch2* recombinant provirus was a novel, truncated 65- to 70-kD Notch2 protein that was targeted to the cell nucleus. This virally encoded Notch2 protein, which resembles previously constructed, constitutively activated forms of Notch, was apparently expressed from a subgenomic transcript spliced at the normal envelope donor and acceptor sequences. The data reported here implicate a nuclear, activated Notch2 protein in FeLV-induced leukemogenesis.

The *Notch* gene was first identified in *Drosophila melanogaster*, in which it has been shown to be involved in a wide variety of cell fate decisions throughout development. *Notch* is thought to encode a receptor molecule that receives signals that delay or block the differentiation of an uncommitted cell, and related genes have been found in a variety of invertebrate and vertebrate organisms (reviewed in references 1 and 11). All *Notch* gene family members encode (i) repeated motifs and conserved cysteines in the extracellular domain and (ii) ankyrin-like repeats, flanked by two potential nuclear localization signals (NLS), in the intracellular domain. Of the three mammalian homologs that have been cloned (13, 23, 26, 27, 46, 53, 61, 62), *Notch1* has the highest identity to *Drosophila Notch*, and in studies of targeted disruption in mice, it has also been shown to play an essential role in development (56). The other two mammalian homologs, *Notch2* and *Notch3*, share significant conservation of structure with *Notch1* (34), but their functions are unknown.

Certain mutations in the intracellular ankyrin repeats of *Drosophila Notch* and murine *Notch1* abolish Notch signaling, which suggests that this region is a key functional domain (20, 22, 32, 47). Studies of engineered *Notch* mutants have established that absence of the extracellular domain, which is thought to allow regulation through ligand binding, can lead to constitutive activation of the intracellular signaling domain. Consistent with this hypothesis, such activated receptors suppress differentiation, leading to the proliferation of one cell lineage at the expense of another (reviewed in references 1 and 17). Interestingly, *Notch* rearrangements similar to these deletion constructs have been correlated with neoplasia. Specifically, translocations at the human *Notch1* locus (TAN-1) that interrupt the gene at the C-terminal end of the extracellular domain and lead to expression of truncated *Notch1* mRNAs are associated with acute lymphoblastic leukemias (9). In addition, the gene *int-3*, which encodes sequences that are distantly related to the intracellular domain of Notch, is interrupted by proviral insertion in mouse mammary tumor virus-associated tumors (48). Moreover, mice transgenic for this disrupted locus develop malignancy (21). Furthermore, all three human *Notch* homologs map to chromosomal regions associated with neoplastic translocations (28), although the natures of these rearrangements, other than disrupted TAN-1, have not been defined.

The transduction and expression of cellular genes by retroviruses has long been appreciated as straightforward and compelling evidence of oncogenic function (reviewed in references 6 and 60). Historically, feline leukemia virus (FeLV), a retrovirus that causes tumors in cats (18), has been an important model for understanding the mechanisms of neoplasia in an outbred mammalian species. Indeed, the acquisition of c-*fes* by FeLV in a naturally occurring tumor was among the earliest examples of oncogene transduction by a mammalian retrovirus (51). Since then, many other examples of recombinant FeLVs harboring host sequences (e.g., *abl*, *sis*, K-*ras*, *fgr*, *fms*, and *kit*) have been documented from natural feline fibrosarcomas (reviewed in references 4, 39, and 40). Additionally, recombinant FeLVs have been cloned from natural thymic lymphosarcomas; there are numerous examples of FeLVs encoding sequences from the c-*myc* proto-oncogene (7, 8, 30, 37, 39, 41, 52) and one example of an FeLV that had transduced the feline T-cell receptor β chain (TCRβ) locus (*tcr*) (14). The presence of a recombinant provirus in an FeLV-induced tumor is strongly correlated with the ability of that recombinant to induce malignancy; in fact, in all but one case tested, these recombinant FeLVs were shown to cause tumors similar to the ones from which they were isolated (3, 5, 15, 29, 35, 43, 51, 57). In this report, we describe the isolation and characterization of FeLV/*Notch2* recombinant genomes from the thymic lymphomas of two cats experimentally infected with a molecularly

* Corresponding author. Mailing address: Department of Microbiology, Box 357242, University of Washington, Seattle, WA 98195. Phone: (206) 543-3146. Fax: (206) 543-8297. Electronic mail address: overbaug@u.washington.edu.

cloned, replication-competent FeLV (FeLV-61E [61E]). The Notch2-encoding sequences in these proviral genomes are structurally similar to activated *Notch* constructs as well as spontaneously rearranged *Notch* family members that are associated with malignancy. Moreover, a novel, nuclear form of this protein is expressed from the FeLV/*Notch2* recombinant provirus.

MATERIALS AND METHODS

Southern blot analysis. Total genomic DNA from cat tissues and cell lines was isolated by standard methods. DNA was digested with restriction endonucleases, electrophoresed through 1% agarose, and transferred to nitrocellulose filters, which were hybridized at high stringency by standard methods to ^{32}P-labeled probes and subjected to autoradiography. For analysis of the TCRβ locus, 15 μg of DNA was digested with *Hin*cII and probed with the 390-bp *Bgl*II fragment of plasmid pFeCβ3, which was derived from the feline Cβ domain of v-*tcr* (14, 57). To detect recombinant FeLV/*Notch2* proviruses, 10 μg of DNA was digested with *Kpn*I and hybridized with the fNotchAA probe described below.

PCR detection and subcloning of FeLV/*Notch2* recombinants. All proviral clones were derived from tumor genomic DNA of two cats that were inoculated with 61E (49). In this report, the nucleotide sequence numbers of the recombinants will be referred to by their corresponding nucleotide numbers in 61E (GenBank accession no. M18247) or rat *Notch2* (GenBank accession no. M93661). FeLV/N2-A^{P} (where P indicates a partial subclone to distinguish it from a similar, full-length provirus [see below]) was amplified by PCR from cat 40836 tumor DNA and cloned into M13mp18 as described for other FeLV partial proviral clones (49). The PCR primers used were FeLV-pol-5 (sense primer spanning 61E nucleotides [nt] 6023 to 6041) and FeLV-U3-2B (antisense primer spanning 61E nt 8189 to 8210) (49). FeLV/N2-C^{P} was cloned from cat 40681 tumor DNA in a similar manner, but the insert was amplified by using a different sense primer that binds to sequences upstream in the polymerase (*pol*) gene (FeLV-pol-1; 5′ AACCAAGAACCTCGAGCCACGG, spanning 61E nt 5807 to 5828). Recombinant genomes were also detected by using a sense *Notch2* primer (Wo9-A; 5′ GGGAGTTATCATGGCGAAAC, spanning rat *Notch2* nt 5595 to 5614) and FeLV-U3-2B. For all primer combinations, PCR amplification conditions were as described previously for FeLV-pol-5 and FeLV-U3-2B (49). The PCR product was electrophoresed, stained with ethidium bromide, visualized under UV, Southern blotted as described above, and hybridized with the ^{32}P-labeled fNotchAA. This probe was amplified from the FeLV/N2-A^{P} PCR clone by using primers Wo9-A and Rev-Wo9A (5′ GCG*TCTAGA*CAGCATCA GTGGGGTGCAC, an antisense primer spanning rat *Notch2* nt 5994 to 6012; italics indicate an *Xba*I restriction site tail).

Molecular cloning of full-length recombinants and derivative constructs. Full-length proviral recombinants FeLV/N2-A and -B were isolated from a library prepared from cat 40836 thymic tumor genomic DNA as described previously (44). Briefly, total genomic DNA was digested with the restriction endonuclease *Eco*RI and ultracentrifuged in a sucrose gradient, and 8- to 20-kb fragments were cloned into *Eco*RI-digested Lambda DASH II vector arms (Stratagene). The library was screened with both an exogenous FeLV long terminal repeat (LTR)-specific probe (exU3 [38]) and probes derived from the *Notch2* sequence of the partial FeLV/N2-A^{P} PCR clone: (i) probe fNotch2AA, described above, and (ii) probe Wo9N/N, which is an approximately 0.5-kb *Nco*I fragment digested from the FeLV/N2-A^{P} PCR clone that spans rat *Notch2* nt 5873 to 6436. Both full-length recombinant proviruses and their host genomic flanking sequences were subcloned into the *Eco*RI site of pUC18 for all further manipulations. The nucleotide sequences of the *Notch2* insertions of all four recombinants were determined by standard protocols, using the chain termination method (50).

FeLV/N2-B-myc was constructed by cloning the *Hin*cII-*Sma*I fragment of the MT6-T six-Myc tag construct (modified to contain a stop codon at the *Eco*RI site) into an intermediate subclone (3′NN) of FeLV/N2-B at the unique *Nsi*I site (61E nt 7800), which had been converted to blunt ends by using the Klenow fragment of *Escherichia coli* DNA polymerase. The intermediate subclone 3′NN consisted of the 3′ half of FeLV/N2-B (spanning from *Xho*I [61E nt 5818] to the *Xba*I site in the 3′ pUC18 polylinker) in pBluescript II SK+ vector. Δenv-FeLV/N2-B-myc was constructed by cloning the *Ppu*MI (rat *Notch2* nt 5481)-to-*Rsr*II (61E nt 7898) fragment of FeLV/N2-B-myc into the *Not*I site of the LacSwitch vector pOPRSVICAT (Stratagene), after the termini of both insert and vector had been converted to blunt ends by using the Klenow fragment. Both constructs were verified by restriction endonuclease digestion and selected nucleotide sequence analysis.

Cell culture. The feline fibroblast cell line AH927 and the feline T-cell line 3201 were maintained as described previously (58), with the addition of 0.25 μg of amphotericin B per ml to the media. The interleukin-2-independent, immortalized cell lines 836-L1 and 836-L2 were derived from the thymic tumor of cat 40836, and their origin and maintenance are described elsewhere (33). 293T cells were maintained in Dulbecco's minimum essential medium supplemented with 10% fetal bovine serum, 100 U of penicillin per ml, 100 μg of streptomycin per ml, 0.25 μg of amphotericin B per ml, and 2 mM L-glutamine.

RT-PCR analysis and cloning of splice junction fragments. A total of 1.5×10^6 293T human embryonic kidney cells were seeded in 10-cm-diameter dishes and were transfected the next day by the calcium phosphate coprecipitation method, using 10 μg of DNA. Total RNA was isolated 40 h posttransfection by using a standard guanidinium isothiocyanate protocol (2). cDNA was generated as follows: diluted RNA was denatured for 10 min at 70°C in the presence of 50 ng of random hexanucleotide primer (Sigma) and chilled on ice, and then reaction cocktail, consisting of 1× first-strand buffer (Gibco BRL), 10 mM dithiothreitol, 0.5 mM all four deoxynucleoside triphosphates, and 3 U of RNase inhibitor (Boehringer Mannheim), was added. Reaction mixtures were incubated for 10 min at 25°C and then at 42°C for 2 min, at which point 200 U of SuperScript II reverse transcriptase (RT; Gibco BRL), or 1 μl of water for minus-RT controls, was added. Reaction mixtures were incubated at 42°C for 50 min and inactivated at 70°C for 15 min.

To amplify cDNA representative of spliced, subgenomic mRNA from FeLV/N2-B, a nested PCR strategy using a combination of FeLV sense and *Notch2* antisense primers was used. For the first round, FeLV-R1 (a sense primer spanning 61E nt 382 to 403 in the R region of the LTR [45]) and RevWo9-B (5′ GCG*TCTAGA*ATATCTGAGCTGCCTCCTCG, an antisense primer spanning rat *Notch2* nt 6022 to 6041; italics indicate an *Xba*I cloning tail) were used. For the second round, FeLV-U5-3 (5′ GCG*GAATTC*GCCGAGGAAGACCCAGT TCG, a sense primer spanning 61E nt 452 to 471; italics indicate an *Eco*RI cloning tail) and RevWo9-A (described above) were used. Two microliters of cDNA reaction product was used as the template in the first round, and 2 μl of first-round product was used as the template in the second round. The reaction mixture was the same as described previously (49) except that the *Taq* polymerase was treated with TaqStart antibody (ClonTech) as recommended by the manufacturer. Both rounds of amplification used thermal cycling conditions described previously (45). The PCR product was electrophoresed through 1% agarose, stained with ethidium bromide, and photographed under UV. To clone the splice junction fragments, products of several PCRs were pooled, and DNA was electrophoresed and gel purified by using standard methods. The 1.2-kb amplification product was digested with the restriction endonucleases *Eco*RI and *Xba*I, whose cleavage sites were present in the primers used in the second-round PCR, and cloned into the same sites of the vector M13mp19, using standard methods.

Δgag-pol-FeLV/N2 is a positive control plasmid that contains an FeLV/N2-B LTR (segment 1) juxtaposed upstream of the 3′ half of FeLV/N2-A^{P} (segment 2) in such a way that the chimeric viral sequences simulate a spliced FeLV/*Notch2* cDNA. Segment 1 begins at a *Hin*dIII site located in the cellular genomic flank upstream of the FeLV/N2-B provirus, ends at the *Bgl*II cleavage site in *gag* (61E nt 1106), and includes the entire 5′ LTR. Segment 1 was ligated to segment 2, which begins at the *Xba*I cleavage site in the *pol* gene (approximately 61E nt 6023; restriction site was in the FeLV-pol-5 cloning tail), ends at the *Eco*RI cleavage site in the 3′ U3 (approximately 61E nt 8210; restriction site was in the FeLV-U3-2B cloning tail), and contains the entire *Notch2* insertion of FeLV/N2-A^{P}. Segment 1 was derived from an intermediate M13mp18 subclone that contained the 5′ LTR and complete 5′ genomic flanking sequences of FeLV/N2-B.

Western immunoblot analysis. 293T cells were transfected as described for RT-PCR analysis (except in the case of the *vpr-myc* expression construct, for which 5 μg was used). Protein extracts were prepared 40 h posttransfection with a lysis buffer consisting of 1% deoxycholic acid, 1% Triton X-100, 0.1% sodium dodecyl sulfate (SDS), 0.15 M NaCl, 0.05 M Tris HCl (pH 7.5), 1 μM leupeptin, 0.3 μM aprotinin, and 500 μM phenylmethylsulfonyl fluoride and incubated for 30 min on ice. Lysates were microcentrifuged at maximum speed for 10 min, and then supernatants were boiled in Laemmli buffer and electrophoresed on an SDS–10% polyacrylamide gel. Western blot analysis and enhanced chemiluminescence detection (Amersham) were performed according to the manufacturer's instructions. The filters were blocked in 5% nonfat dry milk in a solution of 0.5% Tween 20 in Tris-buffered saline (TBS-T). The primary incubation was performed in clarified culture supernatant from a mouse hybridoma secreting anti-Myc monoclonal antibody 9E10 (10), and the secondary incubation was performed in a 1:2,000 dilution of horseradish peroxidase-conjugated monoclonal anti-murine immunoglobulin G antibody. All washes were in TBS-T at room temperature. No specific proteins were detected on similar filters when the analysis was performed without the primary antibody.

Immunofluorescence analysis. Cells were transfected as described for RT-PCR analysis except that 2×10^5 293T cells and 4×10^4 AH927 cells were plated on single-well chamber slides (Nunc), and 5 μg of DNA was coprecipitated. Slides were fixed 40 h posttransfection with 1:1 methanol–acetone-*d*6 for 2 min at −20°C. Immunofluorescence analysis was performed with 9E10 supernatant as the primary antibody and fluorescein-conjugated monoclonal anti-murine immunoglobulin G (1:200 dilution) as the secondary antibody; all washes and incubations were at 4°C in phosphate-buffered saline (PBS). Cells were counterstained with 0.005% Evans blue in PBS for 1 min. Slides were mounted in 0.1% phenylenediamine in 90% glycerol–10% PBS and visualized with a Nikon Optiphot microscope and MRC 600 confocal microscopy attachment using Bio-Rad A1A2 514-nm excitation at the following wavelengths: >600 nm for red (Evans blue) and 520 to 540 nm for green (fluorescein). Similar slides analyzed without the addition of primary antibody showed no specific staining.

Nucleotide sequence accession numbers. The nucleotide sequences of *Notch2* insertions of the recombinant proviruses described in this report are available

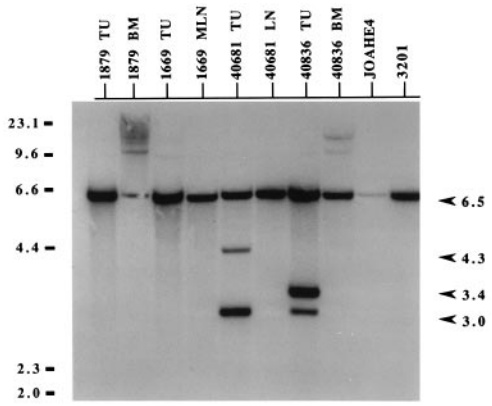

FIG. 1. Southern analysis of FeLV/*Notch2* proviruses in cat tissue DNAs. Ten micrograms of total genomic DNA was digested with *Kpn*I, electrophoresed through 1% agarose, transferred to nitrocellulose, and probed with fNotchAA. Genomic DNAs were derived from cat 1879 tumor (TU) and bone marrow (BM), cat 1669 tumor and mesenteric lymph node (MLN), cat 40681 tumor and lymph node (LN), cat 40836 tumor and bone marrow, JOAHE4 cells, and uninfected 3201 T cells. JOAHE4 DNA was inadvertently underloaded with respect to the other DNAs. Mobility of the molecular weight standards, which are phage lambda DNA cut with *Hin*dIII, are indicated with their corresponding sizes in kilobases on the left. On the right, arrows indicate the positions and sizes of the endogenous *Notch2*-specific fragment (6.5 kb) as well as additional specific fragments in cat 40681 and 40836 tumor DNA.

from GenBank under accession number U47642 through U47645 for FeLV/N2-A (full-length), FeLV/N2-A^P (partial), FeLV/N2-B (full-length), and FeLV/N2-C^P (partial), respectively.

RESULTS

Detection of FeLV/*Notch2* recombinant proviruses in thymic lymphoma DNA. In a survey of proviral genetic variation in tumor DNA from cats inoculated with molecularly cloned FeLV (49), we identified a provirus that had acquired cellular sequences. This recombinant (FeLV/N2-A^P [see Fig. 3c]) was cloned following PCR amplification of the 3′ portion of the viral genome from the DNA of cat 40836 tumor by using the primers FeLV-pol-5 and FeLV-U3-2B. Nucleotide sequence analysis revealed that these cellular sequences were highly related to the rat *Notch2* gene (62), sharing 97% identity at the predicted amino acid level with a portion of the intracellular domain of the protein (see below). To determine whether FeLV/*Notch2* recombinant proviruses were present in other infected cat tissues (49), we prepared a *Notch2*-specific probe (fNotchAA) from FeLV/N2-A^P and used it to analyze DNAs from infected cats by Southern blotting. As shown in Fig. 1, this probe could detect an endogenous *Notch2*-hybridizing *Kpn*I fragment (approximately 6.5 kb) in all feline DNAs examined. We detected two additional fragments (approximately 3.4 and 3.0 kb) in tumor but not in uninvolved DNA from cat 40836. Additionally, there were two additional *Notch2*-specific fragments (approximately 4.3 and 3.0 kb) in DNA from cat 40681 tumor but not in uninvolved DNA, which suggested that this tumor also harbors FeLV/*Notch2* proviruses. Only endogenous *Notch2* was seen in DNA from two other cats (1879 and 1669) that had developed thymic lymphoma, as well as in DNA from uninfected 3201 feline T cells. DNA from the cell line JOAHE4, which is a feline fibroblast cell line chronically infected with 61E that was used to generate the inoculating virus stock for cats 40681 and 40836, showed no evidence of FeLV/*Notch2* proviruses in this analysis (Fig. 1). We used Southern blot analysis to examine the genomic DNA from six additional FeLV-induced tumors of T-cell origin (four naturally occurring and two experimentally induced) but did not detect *Notch2* rearrangement in these samples (data not shown).

To further explore the nature of the FeLV/*Notch2* recombinant genomes in the tumor DNA of cats 40681 and 40836, we performed PCR using a sense *Notch2* primer and an antisense U3 LTR primer and analyzed the products by gel electrophoresis. One prominent fragment (1.6 kb) was seen in cat 40681 tumor but not in uninvolved DNA (Fig. 2A). Three prominent fragments (1.9, 1.7, and 1.5 kb) were seen in tumor DNA from cat 40836 but not in uninvolved DNA from the same animal, suggesting that there was a heterogeneous FeLV/*Notch2* population in this tumor. These fragments hybridized to fNotchAA in Southern analysis (Fig. 2B). We did not detect a specific amplification product(s) in DNA from the negative control, which consisted of 3201 cells that had been transfected with 61E. In agreement with the results shown in Fig. 1, a similar, more sensitive, nested PCR strategy failed to detect FeLV/*Notch2* recombinants in JOAHE4 DNA (data not shown).

Structures and coding capacity of FeLV/*Notch2* recombinant subclones. In our initial PCR amplification of 3′ FeLV fragments with the primers FeLV-pol-5 and FeLV-U3-2B, we detected an FeLV/*Notch2* recombinant (FeLV/N2-A^P) in cat 40836, but we did not detect such a recombinant in cat 40681. However, because Southern and PCR analyses indicated that cat 40681 tumor likely harbored at least one FeLV/*Notch2* proviral genome, we used PCR to amplify a larger fragment from the 3′ half of the FeLV proviruses in cat 40681 tumor. In this manner, we were able to subclone a representative FeLV/*Notch2* provirus with the PCR primer pair FeLV-pol-1 and FeLV-U3-2B, which spans a larger portion of the FeLV genome (FeLV/N2-C^P [Fig. 3g]). Comparison of the nucleotide sequences of the recombinant subclones from both cats revealed similar but not identical structures. In both clones, the transduced *Notch2* sequences were predicted to encode the extreme C-terminal portion of the Notch2 extracellular domain, including the conserved cysteines, as well as the trans-

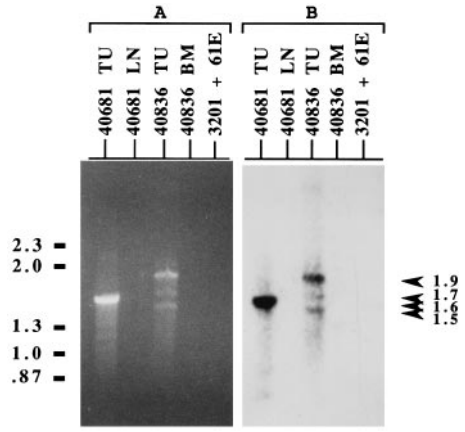

FIG. 2. Detection of FeLV/*Notch2* proviruses by PCR. Subgenomic portions of FeLV/*Notch2* recombinant proviruses were amplified with the primers Wo9-A and FeLV-U3-2B. The DNAs used as templates for PCR were 100 ng of genomic DNA from cat 40681 tumor (TU) and lymph node (LN), cat 40836 tumor and bone marrow (BM), and 3201 T cells that had been transfected with molecularly cloned 61E. A mock PCR included in this set of reactions that lacked DNA yielded no fragments (not shown). (A) The PCR product was electrophoresed through 1% agarose and stained with ethidium bromide. (B) The gel shown in panel A was analyzed by Southern blotting using the fNotchAA probe. For both panels, the mobilities of the molecular weight standards, which are a mixture of phage lambda DNA cut with *Hin*dIII and phage ϕX174 cut with *Hae*III, are indicated with their corresponding sizes in kilobases on the left.

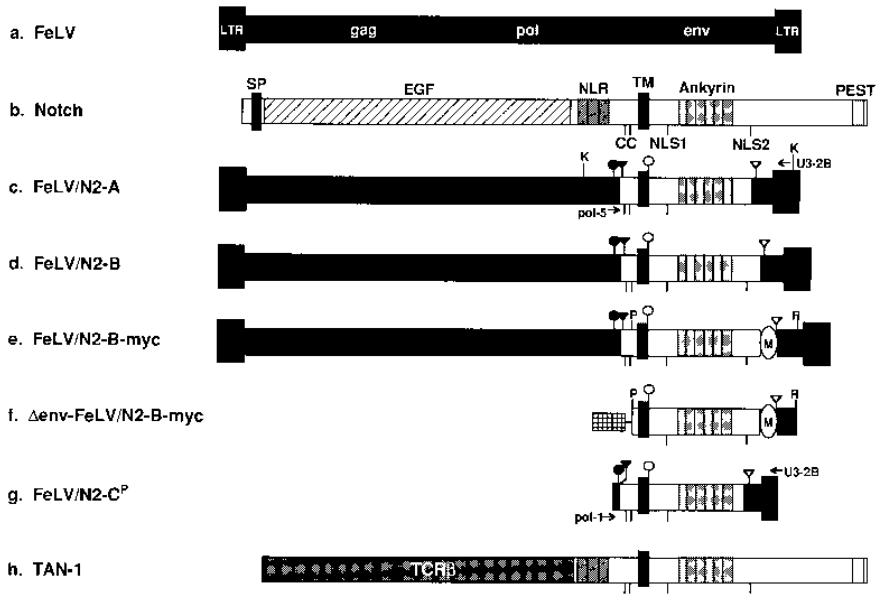

FIG. 3. Structures of FeLV/*Notch2* recombinants. Black boxes indicate FeLV sequences, and open boxes, superimposed by relevant domains, indicate Notch sequences. (a) Schematic FeLV provirus, showing the positions of the LTR sequences as well as the genes *gag*, *pol*, and *env*. (b) Schematic Notch protein structure: SP, signal peptide; EGF, epidermal growth factor-like repeats; NLR, *notch*/*lin12* repeats; C, conserved cysteines; TM, transmembrane domain; ankyrin, ankyrin-like repeats; NLS, nuclear localization signal; PEST, PEST motif. (c) FeLV/N2-A recombinant, representative of both partial PCR clone FeLV/N2-A^P as well as a full-length proviral clone isolated from cat 40836, which differ by only a single amino acid in their Notch2 sequences. The normal FeLV envelope initiation codon is indicated by a filled circle. The first stop codon that occurs in this reading frame is in the *Notch2* sequence and is indicated by a black triangle. The putative initiation codon in *Notch2* (MET-79) is indicated by an open circle, and the first downstream stop codon in this reading frame, which is in the viral envelope TM domain, is indicated by an open triangle. The primers used to amplify FeLV/N2-A^P are indicated with arrows. The *Kpn*I sites (61E nt 4895 and 8336) diagnostic for fNotchAA Southern analysis (Fig. 1) are shown (K). *Kpn*I is not predicted to cut within the *Notch2* sequences. (d) FeLV/N2-B, a full-length proviral clone from cat 40836. (e) FeLV/N2-B-myc, a derivative of FeLV/N2-B with a Myc epitope tag (M) inserted in frame at 61E nt 7800, downstream of the 3′ transduction junction. (f) Δenv-FeLV/N2-B-myc, a derivative of FeLV/N2-B-myc beginning at truncated Notch2 codon 38 (P, *Ppu*MI site) and ending at 61E nt 7898 (*R*, *Rsr*II site), cloned into LacSwitch, a eukaryotic expression vector driven by the Rous sarcoma virus LTR promoter (hatched box) that lacks its own initiation codon. (g) FeLV/N2-C^P, a PCR-derived partial proviral clone from cat 40681. The primers used to amplify this subclone are indicated with arrows. (h) For the purpose of comparison, a schematic structure of the rearranged human TAN-1 locus (9) is presented.

membrane domain, the first NLS, and the entire ankyrin repeat region of the intracellular domain.

In FeLV/N2-A^P (Fig. 3c), the *Notch2* sequences were positioned downstream of the initiating methionine codon (MET-env) for the viral envelope protein (Env), within the sequences encoding the FeLV Env signal peptide leader. The 5′ transduction junction was such that the *Notch2* open reading frame (ORF) was out of frame with respect to the *env* ORF. As a result, there was a termination codon in the *env* ORF four nucleotides into the *Notch2* sequences. However, in the *Notch2* reading frame itself, there were no translational stop codons. The 3′ transduction junction occurred within, and disrupted, the normal termination codon for the FeLV envelope transmembrane protein (TM) such that the *Notch2* ORF would terminate several nonsense amino acids thereafter. The structure of FeLV/N2-A^P was consistent with the most prominent fNotchAA-hybridizing *Kpn*I fragment (3.0 kb) seen in Southern analysis of cat 40836 tumor DNA (Fig. 1 and 3c). This structure is also consistent with the 1.5-kb fragment PCR amplified by the primers Wo9-A and FeLV-U3-2B (Fig. 2).

In FeLV/N2-C^P (Fig. 3g), the Notch2-encoding sequences were predicted to be 98% identical to those of rat *Notch2* at the amino acid level. The transduced sequence began at the same site in *Notch2* as in FeLV-N2-A^P, but the insertion was positioned further upstream in the *env* gene, four nucleotides downstream of MET-env. This structure explains our inability to amplify this FeLV/*Notch2* recombinant from cat 40681 tumor with the primer FeLV-pol-5, because the primer binding site is further downstream in *env*. In the *env* reading frame, there was a termination codon in the *Notch2* sequence four nucleotides downstream of the 5′ transduction junction. However, the *Notch2* ORF was open until after the 3′ transduction junction, which was located near the end of the TM coding sequences. The stop codon for the *Notch2* ORF was a nonsense TM codon several nucleotides downstream of the junction. Although the *Notch2* insertion was 32 nt shorter than that of FeLV/N2-A, it still contained the entire ankyrin repeat domain. As with FeLV/N2-A^P, the structure of FeLV/N2-C^P was consistent with the 3.0-kb *Kpn*I fragment seen in Southern analysis of 40681 tumor DNA in Fig. 1. Moreover, the structure of FeLV/N2-C^P was also consistent with the 1.6-kb fragment detected by PCR with the primers Wo9-A and FeLV-U3-2B (Fig. 2).

Molecular cloning of full-length FeLV/*Notch2* genomes. To further delineate the structures of the recombinant proviruses, we cloned full-length representative proviral genomes. We focused on cat 40836 tumor DNA because of the heterogeneity that we had detected in the FeLV/*Notch2* provirus population by PCR (Fig. 2). We isolated two full-length FeLV/*Notch2* proviruses from a genomic library of cat 40836 tumor and analyzed the nucleotide sequences of the transduced sequences. One recombinant was virtually identical to FeLV/N2-A^P (FeLV/N2-A [Fig. 3c]), possessing the same transduction junctions and differing by only one predicted amino acid in the Notch2-encoding sequences. The second recombinant (FeLV/N2-B [Fig. 3d]) contained a region of *Notch2* that was 149 nt longer than that of FeLV/N2-A, such that it encoded the second potential NLS sequence found in *Notch* family mem-

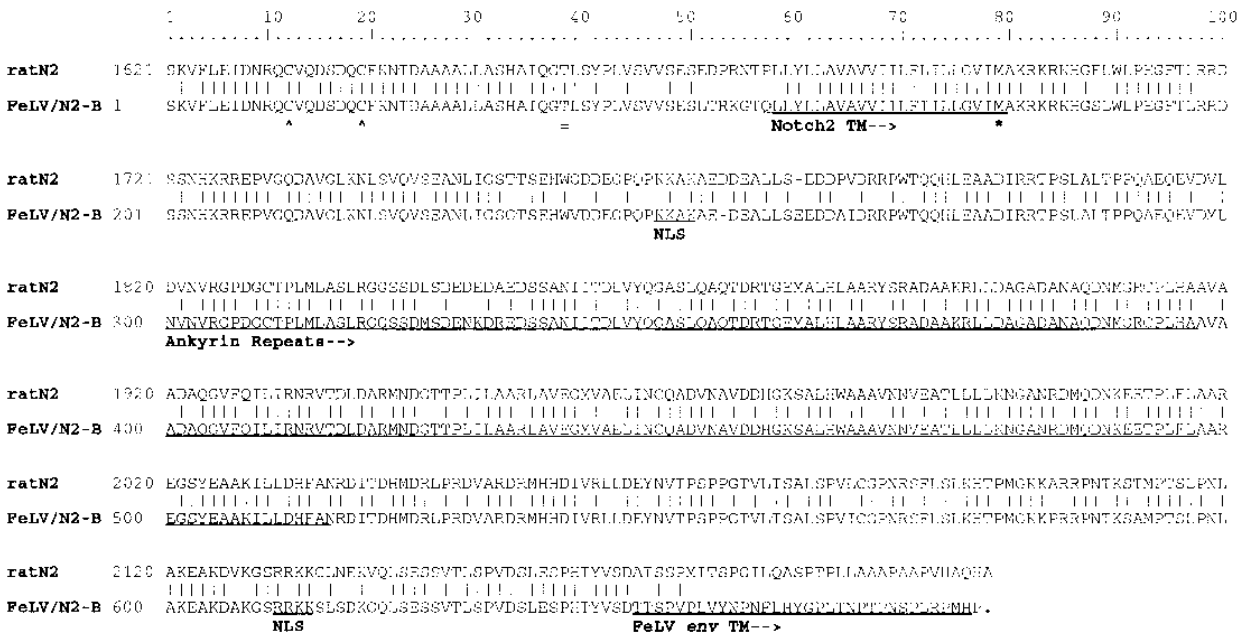

FIG. 4. Comparison of the predicted amino acid sequences of rat *Notch2* (ratN2) and FeLV/N2-B. Truncated Notch2 numbering begins (at position 1) at the first common amino acid of the transduced region; vertical lines indicate identity. Dashes indicate gaps that were introduced to facilitate alignment. The dot at the end of the FeLV/*Notch2* sequence indicates a termination codon. Motifs of interest are underlined (Notch2 TM, NLS, ankyrin repeats, and FeLV envelope TM sequences); also indicated are conserved cysteines (carats), MET-79 (marked with an asterisk) and the first codon after the *Ppu*MI cleavage site used to create Δenv-FeLV/N2-B-myc (double underlined).

bers. In Fig. 4, the predicted amino acid sequence of this longest Notch2-encoding insertion is aligned with that of rat Notch2; the two sequences exhibit 96% identity. The 5′ transduction junction was identical to that of FeLV/N2-A and -A^P, but the 3′ junction differed; it was located near the end of FeLV TM, and a stop codon in the *Notch2* ORF occurred in TM, 30 nonsense amino acid codons downstream of this junction. The configuration of this recombinant provirus was consistent with the approximately 3.4-kb *Kpn*I fragment seen in Southern analysis of cat 40836 tumor DNA (Fig. 1) as well as with the 1.9-kb fragment detected by PCR with the primers Wo9-A and FeLV-U3-2B (Fig. 2).

Nucleotide sequences at the transduction junctions. We examined specific nucleotide sequences at the transduction junctions of FeLV/N2-A, -B, and -C^P to determine whether there was evidence of homology that may have facilitated recombination. For FeLV sequences, 61E was used as the parental reference. Rat *Notch2* was used as the parental reference sequence for the transduced *Notch2* sequences, except in the case of the 3′ junctions of FeLV/N2-A and -C^P, for which we were able to use the longer FeLV/N2-B as the feline *Notch2* parental reference sequence. As shown in Fig. 5, there were seven nucleotides of perfect homology (CGGCCCA) at the 3′ junction of FeLV/N2-C^P and misaligned homology (TCCCCC) very near the 3′ junction of FeLV/N2-B (underlined in Fig. 5). The other junctions had only a single homologous nucleotide at the junction, a G residue (all 5′ junctions) or an A residue (FeLV/N2-A 3′ junction). Interestingly, the 5′ transduction junctions of FeLV/N2-A and -B contained a direct repeat nonamer (GTGTTTCTG) separated by seven nucleotides (underlined in Fig. 5). We saw no evidence for consensus ACCCC signals or other *cis* sequences proximal to the junctions, as discussed by Doggett et al. (8), with the exception of marked pyrimidine strand bias at or near five of six of the junctions (boldface in Fig. 5). While the three 5′ junctions occurred in FeLV sequences that bore some resemblance to the eukaryotic splice donor consensus sequence (36), these sequences were not observed to be used as splice donors in a previous analysis (45); moreover, there was little identity with the consensus acceptor motif (36) in the corresponding *Notch2* sequences.

Detection and characterization of subgenomic recombinant RNA species in transfected cells. Northern (RNA) analysis of RNA from cat 40836 tumor, but not uninvolved tissue from the same animal, showed expression of feline *Notch2*-hybridizing RNA, although the tissue RNA was sufficiently degraded to preclude identification of discrete species (data not shown). Because of this, and because of the heterogeneity of the recombinant population in this tissue, we chose to directly examine the expression of cloned FeLV/*Notch2*. Because retroviruses typically make subgenomic mRNAs to express 3′ genes such as *env*, we examined the spliced mRNAs that were expressed from FeLV/*Notch2* proviruses. FeLV/N2-B was chosen for this and all subsequent analyses because it encoded the longest *Notch2* sequence. We were unsuccessful at establishing stable cell lines expressing FeLV/*Notch2* proviruses in feline cells because of apparent toxicity (data not shown). Thus, we isolated total RNA after transient transfection of proviral clones into the human embryonic kidney cell line 293T, which demonstrates a high transient transfection efficiency, and used a nested RT-PCR method to amplify spliced RNAs, using sense 5′ LTR primers and antisense *Notch2* primers. cDNA representing full-length genomic RNA would be predicted to be too large to be detected with this PCR strategy; only one species, corresponding to the size (1.2 kb) predicted for a message spliced from the normal donor to the normal *env* acceptor sequences, was detected (Fig. 6). This signal was evident with 5 μg down to 5 ng of total input of cellular RNA. The nested PCR was sufficiently sensitive to reproducibly detect approximately one copy (10^{-18} g) of the control plasmid

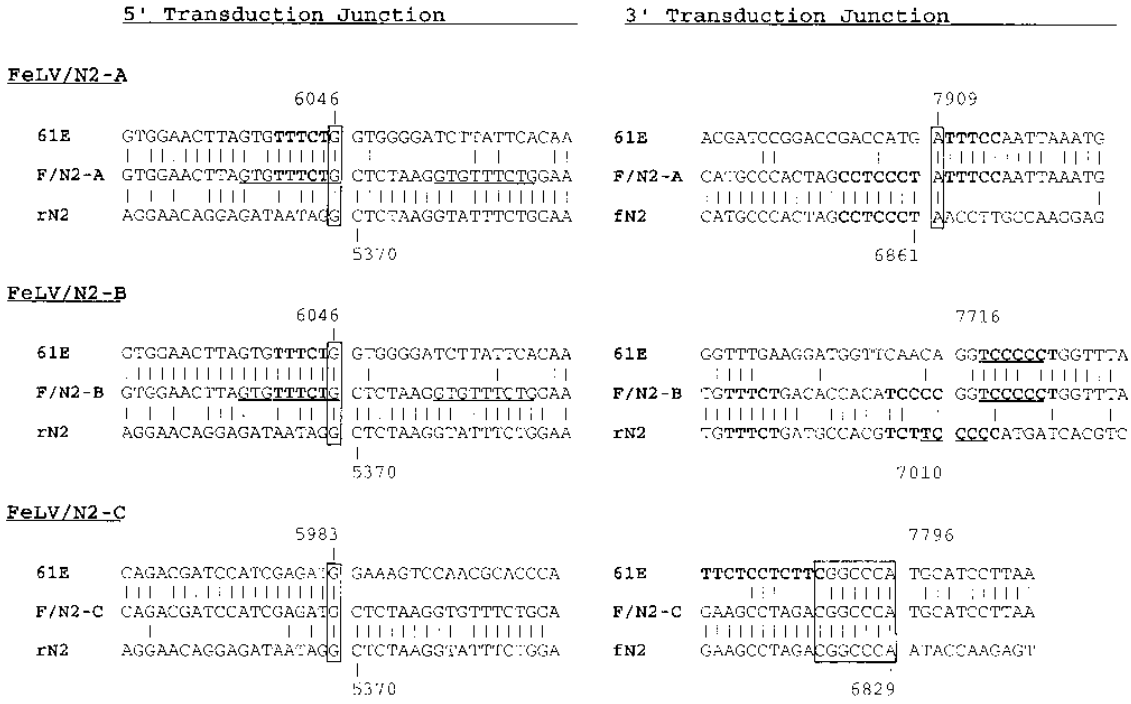

FIG. 5. Nucleotide sequence of FeLV/*Notch2* transduction junctions. In each panel, the top line shows the 61E parental reference sequence, the middle line shows the FeLV/*Notch2* recombinant sequence, and the bottom line shows the parental *Notch2* sequence, either rat *Notch2* (rN2) or FeLV/N2-B (fN2). Vertical lines indicate nucleotide identity. The separation between stretches of nucleotides indicates the presumed recombination breakpoint. Regions of homology or identical single nucleotides at the junction are boxed, and pyrimidine-rich regions are indicated in boldface. A misaligned region of homology at the 3′ junction of FeLV/N2-B is underlined, as is a direct repeat nonamer in the 5′ junction of FeLV/N2-A. For all FeLV recombinants, the nucleotide positions of the transduction junctions are indicated.

Δgag-pol-FeLV/N2 (data not shown), which was constructed to simulate a DNA of the structure and size (1.4 kb) of the predicted *env*-spliced cDNA. To confirm the nature of the splice junction of the mRNA represented by the 1.2-kb RT-PCR amplification product, we cloned this product and determined the partial nucleotide sequences of two independent clones. The splice junctions were identical to the 61E envelope splice junction that was previously determined by our laboratory (45). These results suggested that the Notch2 protein, if expressed, would be initiated internally from a subgenomic message spliced to the normal envelope donor and acceptor sequences and not from an RNA alternatively spliced into *Notch2*.

Protein expression from a full-length FeLV/*Notch2* provirus in transfected cells. To directly examine whether a Notch2 protein product was encoded by the proviral genome, we engineered a Myc epitope tag into the C-terminal flanking sequences downstream of *Notch2* in FeLV/N2-B (FeLV/N2-B-myc [Fig. 3e]) and performed Western analysis after transient transfection into 293T cells. As shown in Fig. 7 (lane 3), an approximately 65- to 70-kDa protein was detected in total lysates from cells transfected with FeLV/N2-B-myc when probed with a monoclonal antibody against the Myc epitope tag. The protein was not seen in untransfected cells or in cells transfected with FeLV/N2-B lacking the tag (Fig. 7, lanes 1 and 2). Thus, a truncated Notch2 product extending all the way to the C-terminal tag can be translated in the context of the recombinant provirus. Because RT-PCR analysis suggested that only *env*-spliced subgenomic mRNA is made, we inspected the 5′ *Notch2* region for sequences that might promote internal initiation. The first available methionine codon (MET-79) in the *Notch2* sequences, which is present near the boundary of

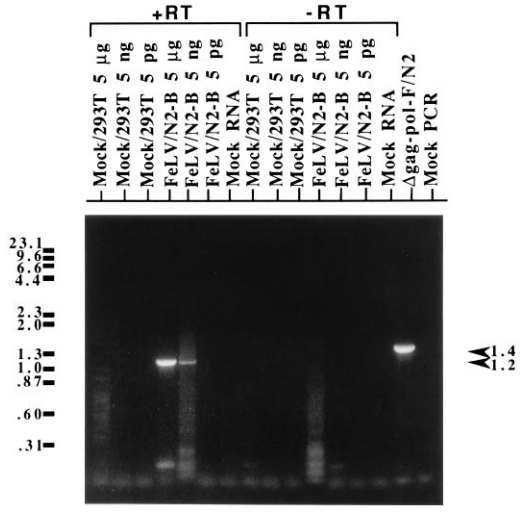

FIG. 6. RT-PCR analysis of 293T RNA transiently transfected with FeLV/*Notch2*. PCR products were electrophoresed through 1% agarose and visualized with ethidium bromide under UV. A representative result is shown. Mock/293T lanes contain RNA from mock-transfected cells; FeLV/N2-B lanes contain RNA from cells transfected with this construct. The amount of input RNA is noted after the lane designation. cDNA synthesis reactions that contained RT are designated +RT. To ensure that positive signals were derived from RNA instead of residual DNA from the transfection, a set of reactions was incubated without RT (−RT). cDNA reactions that contained water instead of RNA are labeled Mock RNA, and a PCR control using water as template is labeled Mock PCR. The positive control plasmid Δgag-pol-FeLV/N2 was also included. The mobilities of the molecular weight standards, which are the same as in Fig. 2, are indicated with their corresponding sizes in kilobases on the left. On the right, arrows indicate the sizes and mobilities of the 1.4-kb Δgag-pol-FeLV/N2 amplification product and the 1.2-kb spliced cDNA amplification product.

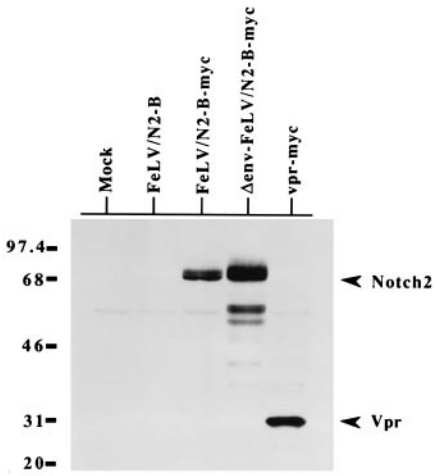

FIG. 7. Expression of FeLV/Notch2 proteins in transiently transfected 293T cells. A representative Western blot analysis of cells transfected with no DNA (mock; lane 1), FeLV/N2-B (lane 2), FeLV-N2-B-myc (lane 3), Δenv-FeLV/N2-B-myc (lane 4), or the positive control human immunodeficiency virus type 1 *vpr-myc* (lane 5), probed with anti-Myc epitope antibody, is shown. The mobility of the enhanced chemiluminescence protein molecular weight markers (Amersham) and their corresponding sizes in kilodaltons are indicated on the left.

the transmembrane and intracellular sequences, is in an optimal Kozak translational initiation context (ATC**ATG**G) (25). A Myc-tagged protein initiating at MET-79 would be predicted to be 65 kDa, which is consistent with the approximately 65 to 70 kDa seen in Western analysis.

Because the RT-PCR data suggested that Notch2 was expressed by an internal initiation mechanism, we deleted a portion of FeLV/N2-B-myc including the *env* initiation codon and the first 37 codons of *Notch2* and cloned the remaining *Notch* sequences into a eukaryotic expression vector lacking its own initiation codon (Δenv-FeLV/N2-B-myc [Fig. 3f]). Western analysis of cells transfected with Δenv-FeLV/N2-B-myc detected a specific protein similar in size (65 to 70 kDa) to FeLV/N2-B-myc (Fig. 7, lane 4), as well as smaller products that may be proteolytic breakdown products. This result indicates that expression of Notch2 protein is not dependent on the presence of MET-env and provides further support for internal initiation at *Notch2* MET-79.

Subcellular localization of FeLV/Notch2 protein. To determine the subcellular localization of truncated Notch2 protein, we performed indirect immunofluorescence analysis of 293T cells and feline AH927 fibroblasts transiently transfected with FeLV/N2-B-myc and visualized the cells by confocal microscopy (Fig. 8). Figures 8A and E show fields of AH927 and 293T cells, respectively, transfected with FeLV/N2-B-myc and viewed at a wavelength that detects Evans blue staining of the cytoplasm and nucleoli. Figures 8B and F represent the same fields of cells at a wavelength that detects the fluorescein-isothiocyanate-conjugated antibody staining of the Myc epitope tag, demonstrating strong specific signal in both cell types transfected with FeLV/N2-B-myc. When these images were merged, it was clear that the localization of the Myc-tagged Notch2 protein was exclusively nuclear in both cell types (Fig. 8C and G). No specific staining was seen in mock-transfected cells (Fig. 8D and H).

Clonal TCRβ locus rearrangement in tumors and derived cell lines. To confirm the thymocyte origin and clonality of the thymic lymphomas from cats 40681 and 40836, we analyzed the configuration of the TCRβ locus by Southern blot analysis with

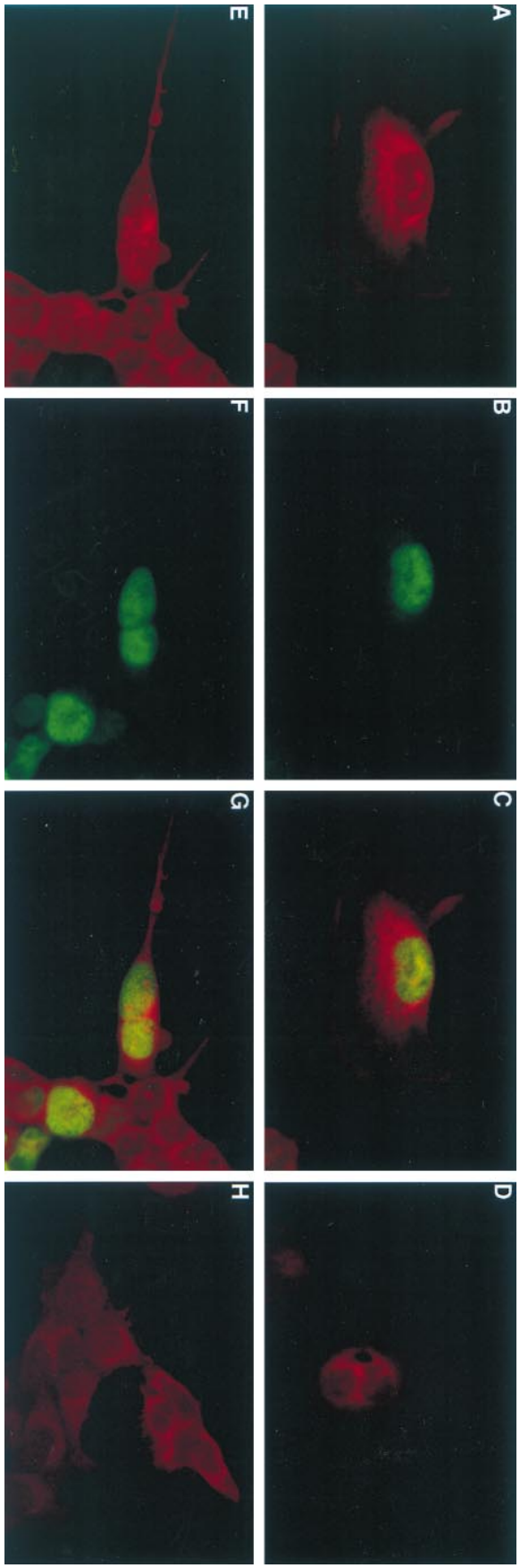

FIG. 8. Subcellular localization of FeLV/N2-B-myc protein. Shown are immunofluorescence analysis and confocal microscopy of transiently transfected AH927 feline fibroblasts (A to D) and human 293T embryonic kidney cells (E to H). (A and E) Evans blue staining of the cytoplasm of cells transfected with FeLV/N2-B-myc; (B and F) same fields at a wavelength to detect fluorescein (Myc-tagged protein); (C and G) computer merge of panels B and F; (D and H) mock-transfected cells, merge of Evans blue and fluorescein wavelengths.

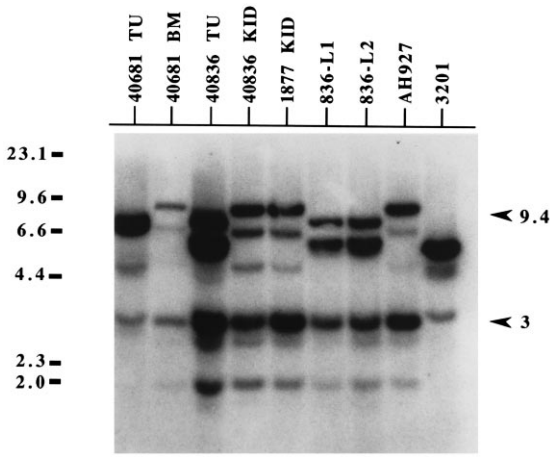

FIG. 9. Southern blot analysis of the TCRβ locus in feline cells. Fifteen micrograms of total RNA was digested with *Hin*cII, electrophoresed in 1% agarose, transferred to nitrocellulose, hybridized with a probe derived from the Cβ domain of v-*tcr* (14, 57), and subjected to autoradiography. Tissue genomic DNAs were derived from cat 40681 tumor (TU) and bone marrow (BM), cat 40836 tumor and kidney (KID), and cat 1877 kidney. In addition, cell line DNA was analyzed: 836-L1 and 836-L2 (both derived from cat 40836 tumor cells [33]), AH927 feline fibroblasts, and 3201 feline T cells. The mobilities of the molecular weight markers, which are the same as in Fig. 1, and their corresponding sizes in kilobases are indicated on the left.

a Cβ-specific probe (14, 57). As described previously, digestion of the gene with the restriction endonuclease *Hin*cII will generate a 9.4-kb Cβ1 fragment and a 3-kb Cβ2 fragment when the locus is in the germ line configuration (57, 59). As shown in Fig. 9, six fragments were seen in DNA from feline germ line control cells (AH927), including the predicted 9.4- and 3-kb species. The additional fragments evident on this long exposure are probably related germ line species that overlap with a small region of the probe. In contrast, DNA from a clonal T-cell tumor line (3201) contained a unique rearrangement at this locus (57). When cat tissue DNAs were analyzed, it was evident that tumor DNA from both cats 40681 and 40836 manifested a unique rearrangement in this locus, while germ line configuration was seen in uninvolved tissue DNA from these cats, as well as in kidney DNA from control cat 1877, which was euthanized after a nonmalignant wasting disorder (49). A pattern of rearrangement identical to that of cat 40836 tumor was also seen in two continuous cell lines (836-L1 and 836-L2 [33]) derived from this cat at necropsy. Thus, both tumors were of clonal thymocyte origin. Additionally, analysis of the cell surface expression of various lymphocyte surface markers on cat 40836 primary tumor cells as well as 836-L1 and -L2 cells indicated that this tumor arose from a mature $CD4^+$ thymocyte (33).

DISCUSSION

The mechanism of FeLV-mediated oncogenesis is likely multifactorial and is thought to involve both host and viral determinants (40). Specific viral sequences and/or proteins probably contribute, as well as insertional mutagenesis and transduction of host proto-oncogenes by the infecting provirus. While numerous FeLV recombinant genomes bearing cellular sequences have been isolated from natural feline tumors (reviewed in reference 40), this report describes the first example of FeLV having transduced an unrelated host cell gene in an experimental infection. Moreover, the recombinant FeLVs described here represent the first reported instance of the transduction of a Notch family member. All recombinant proviruses, either PCR subclones or full-length proviral clones, contained host-derived sequences encoding a portion of the intracellular domain of Notch2 that includes the ankyrin repeats. The structure of this rearranged *Notch2* gene is provocative because of its similarity to activated *Notch* mutant constructs (reviewed in reference 1), as well as to rearranged human *Notch1* (TAN-1) that has been associated with malignancy (9). Our results clearly demonstrate that truncated Notch2 protein is expressed from an FeLV/*Notch2* recombinant provirus; as such, they represent the first report of protein expression from a rearranged mammalian *Notch* homolog.

We characterized four recombinant proviruses from two cats, three of which were unique in structure. The 3′ transduction junction of FeLV/N2-C^P contained seven nucleotides of perfect homology, which is most consistent with a model (reviewed in reference 63) whereby these *Notch2* sequences were acquired by template switching during reverse transcription of copackaged wild-type FeLV and an FeLV/*Notch2* readthrough RNA transcript. Four of the five other transduction junctions, including the 5′ junction of FeLV/N2-C^P, contained only one common residue between FeLV and *Notch2*; in this regard, they are similar to some naturally occurring recombinant proviruses (63). Similar lack of homology has also been observed at the junctions of a subset of recombinants characterized in in vitro systems in which recombination was attributed to a RT-mediated template switching mechanism (e.g., references 55 and 64). Because all of the recombinants have the same 5′ *Notch2* junction, it is possible that this particular region of *Notch2* sequence is a favored site for RT-mediated recombination. However, a more intriguing hypothesis is that there is a strong selective pressure to retain these particular sequences for optimal expression of the downstream cistron. Because the two clones from cat 40836, FeLV/N2-A and -B, possess identical 5′ junctions but differ at the 3′ recombination point, we speculate that FeLV/N2-A evolved from the longer FeLV/N2-B as a result of an additional recombination event during reverse transcription; it remains to be elucidated whether these proviruses are biologically distinct.

Several pieces of data implicate a methionine codon at the boundary of the Notch2 TM and intracellular domain (MET-79) as the initiation codon for truncated Notch2 protein despite the fact that it is located downstream of MET-env: (i) the construct Δenv-FeLV/N2-B-myc, which lacks MET-env and *env* sequences, nevertheless was able to express truncated Notch2; (ii) MET-79 is the first available methionine codon in Δenv-FeLV/N2-B-myc; (iii) MET-79 is in an optimal Kozak consensus context; and (iv) the sizes of the proteins expressed by FeLV/N2-B-myc and Δenv-FeLV/N2-B-myc are the same (approximately 65 to 70 kD) and consistent with the size of 65 kDa predicted for a Myc-tagged protein initiating at MET-79 from these constructs. Because the RT-PCR results suggest that an mRNA alternatively spliced into *Notch2* sequences was not expressed, we believe that internal initiation within *Notch2* sequences is the most likely mechanism of truncated Notch2 translation. Reinitiation of eukaryotic translation at the next available methionine that is in an optimal context and that is downstream of a termination codon (as is MET-79) has been shown to occur efficiently with artificial constructs (24) and with a number of viral and cellular genes (25). Alternatively, there is a long polypyrimidine-rich tract and predicted secondary structure upstream of MET-79 (data not shown) which is characteristic of some internal ribosomal entry sites (19).

Analyses of *Drosophila Notch* mutant constructs have shown that not all extracellular domain deletions of the Notch protein have the same phenotype. For example, while a truncated

protein that retained the conserved cysteines and the transmembrane domain in addition to the intracellular portion was essentially nonfunctional in an in vivo activity assay, removal of a region including the cysteines and the transmembrane domain resulted in a protein with a dominant gain-of-function or activated phenotype (32). Thus, our data with Δenv-FeLV/N2-B-myc, which effectively rule out the possibility of a longer Env/Notch fusion product containing the conserved cysteines and transmembrane domain, are significant because they show that the structure of FeLV/Notch2 protein is similar to that of an activated form of Notch.

The Notch2 protein expressed by FeLV/N2-B is localized to the nucleus in both cell types examined, which is consistent with a protein predicted to contain NLS sequences and to lack a transmembrane anchor. Protein products of engineered, constitutively active *Notch* constructs lacking the extracellular domain are also targeted to the nucleus (12, 20, 22, 32, 42, 47, 54). Although nuclear localization of wild-type Notch in vivo has not been demonstrated conclusively in normal cells, several groups have suggested that nuclear localization is correlated with the constitutive activity of *Notch* deletion constructs, and further, that wild-type *Notch* signaling might require a cleavage and nuclear translocation event (reviewed in references 1 and 16). This model was supported by a recent report in which an activated mouse *Notch1* construct was shown to bind directly to a nuclear transcription factor concurrent with transactivation of the HES-1 promoter, thus bypassing a cytoplasmic signaling cascade (20). Given these data, it is possible that nuclear localization potentiates any intrinsic signaling activity of FeLV/*Notch2* and its potential binding partners.

On the basis of historical correlation between retroviral transduction and tumorigenesis, as well as the phenotype of activated *Notch* mutants, we predict that the altered form of *Notch2* described here functioned as an oncogene in lymphocyte malignancy. The normal role of *Notch2* in the cell is unknown, but extrapolating from studies of *Drosophila Notch* and mammalian *Notch1*, we hypothesize that a dominant, constitutively active nuclear form of the protein expressed from the FeLV provirus would bypass signaling by its normal ligand and alter the pattern of gene expression to delay differentiation. This delay could facilitate transformation by blocking the target lymphocyte in a proliferative stage. Such a block might be similar to the mechanism of action postulated for other FeLV-activated genes (e.g., *myc*) in feline thymic lymphoma, whereby transformation may occur in a window of sensitivity that is temporally proximal to TCRβ rearrangement, perhaps as a result of the prevention of normal apoptotic elimination of self-reactive cells (57, 59). Because the formation of thymic lymphoma in these cats likely required a secondary event(s) in addition to a retrovirally activated Notch2 protein, our system will function as a unique and powerful tool to identify *Notch2*-collaborating genes, which can be elucidated by the analysis of loci that are rearranged by proviral integration into thymic tumor DNA. Indeed, a rearrangement of *bmi-1*, which encodes a nuclear protein with domains characteristic of the zinc finger class of transcription factors, has already been identified in cat 40681 tumor (31). Such studies will be a first step in clarifying the signaling pathway downstream of *Notch2* in lymphocyte development and *Notch2*-associated oncogenesis.

ACKNOWLEDGMENTS

We thank Michael Emerman and Vineet KewalRamani for providing 9E10 culture supernatant and the *vpr-myc* expression construct, Mark Roth for providing the MT6-T Myc epitope construct, Vineet KewalRamani for introducing the stop codon into MT6-T, James Neil for providing the pFeCβ3 construct, Laura Levy for supplying certain cat tissue DNA samples, and Paul Goodwin for technical assistance with confocal microscopy. Additionally, we thank Raphael Kopan, Edward Giniger, Laurie Milner, A. Dusty Miller, Michael Emerman, Vineet KewalRamani, and members of our laboratory for helpful discussion and Edward Giniger and Maxine Linial for critical review of the manuscript.

This research was supported by NIH grant CA51080. Additionally, J.O. is a Scholar of the Leukemia Society of America, and J.L.R. is a recipient of a Helen Riaboff Whitely Graduate Fellowship Award.

REFERENCES

1. **Artavanis-Tsakonas, S., K. Matsuno, and M. E. Fortini.** 1995. Notch signaling. Science **268:**225–232.
2. **Ausubel, F. M., R. Brent, R. E. Kingston, D. D. Moore, J. G. Seidman, J. A. Smith, and K. Struhl (ed.).** 1987. Current protocols in molecular biology. Greene Publishing Associates and Wiley-Interscience, New York.
3. **Bergold, P. J., J. A. Blumenthal, E. D'Andrea, H. W. Snyder, L. Lederman, A. Silverstone, H. Nguyen, and P. Besmer.** 1987. Nucleic acid sequence and oncogenic properties of the HZ2 feline sarcoma virus v-*abl* insert. J. Virol. **61:**1193–1202.
4. **Besmer, P.** 1983. Acute transforming feline retroviruses. Curr. Top. Microbiol. Immunol. **107:**1–27.
5. **Besmer, P., W. D. Hardy, Jr., E. E. Zuckerman, P. Bergold, L. Lederman, and H. W. Snyder, Jr.** 1983. The Hardy-Zuckerman 2-FeSV, a new feline retrovirus with oncogene homology to Abelson-MuLV. Nature (London) **303:**825–828.
6. **Bishop, J. M.** 1990. Retroviruses and oncogenes II. Biosci. Rep. **10:**473–491.
7. **Braun, M. J., P. L. Deininger, and J. W. Casey.** 1985. Nucleotide sequence of a transduced *myc* gene from a defective feline leukemia provirus. J. Virol. **55:**177–183.
8. **Doggett, D. L., A. L. Drake, V. Hirsch, M. E. Rowe, V. Stallard, and J. I. Mullins.** 1989. Structure, origin, and transforming activity of feline leukemia virus-*myc* recombinant provirus FTT. J. Virol. **63:**2108–2117.
9. **Ellisen, L. W., J. Bird, D. C. West, A. L. Soreng, T. C. Reynolds, S. D. Smith, and J. Sklar.** 1991. TAN-1, the human homolog of the Drosophila notch gene, is broken by chromosomal translocations in T lymphoblastic neoplasms. Cell **66:**649–661.
10. **Evan, G. I., G. K. Lewis, G. Ramsay, and J. M. Bishop.** 1985. Isolation of monoclonal antibodies specific for human c-*myc* proto-oncogene product. Mol. Cell. Biol. **5:**3610–3616.
11. **Fortini, M. E., and S. Artavanis-Tsakonas.** 1993. Notch: neurogenesis is only part of the picture. Cell **75:**1245–1247.
12. **Fortini, M. E., I. Rebay, L. A. Caron, and S. Artavanis-Tsakonas.** 1993. An activated Notch receptor blocks cell-fate commitment in the developing Drosophila eye. Nature (London) **365:**555–557.
13. **Franco del Amo, F., D. E. Smith, P. J. Swiatek, M. Gendron-Maguire, R. J. Greenspan, A. P. McMahon, and T. Gridley.** 1992. Expression pattern of Motch, a mouse homolog of Drosophila Notch, suggests an important role in early post-implantation mouse development. Development **115:**737–744.
14. **Fulton, R., D. Forrest, R. McFarlane, D. Onions, and J. C. Neil.** 1987. Retroviral transduction of T-cell antigen receptor beta-chain and myc genes. Nature (London) **326:**190–194.
15. **Gardner, M. B., R. W. Rongey, P. Arnstein, J. D. Estes, P. Sarma, R. J. Huebner, and C. G. Rickard.** 1970. Experimental transmission of feline sarcoma to cats and dogs. Nature (London) **226:**807–809.
16. **Goodbourn, S.** 1995. Notch takes a short cut. Nature (London) **377:**288–289.
17. **Greenwald, I.** 1994. Structure/function studies of lin-12/Notch proteins. Curr. Opin. Genet. Dev. **4:**556–562.
18. **Hardy, W. D.** 1993. Feline oncoretroviruses, p. 109–180. *In* J. A. Levy (ed.), The Retroviridae, 2nd ed. Plenum Press, New York.
19. **Jackson, R. L., S. L. Hunt, J. E. Reynolds, and A. Kaminski.** 1995. Cap-dependent and cap-independent translation: operational distinctions. Curr. Top. Microbiol. Immunol. **203:**1–30.
20. **Jarriault, S., C. Brou, F. Logeat, E. H. Schroeter, R. Kopan, and A. Israel.** 1995. Signalling downstream of activated mammalian Notch. Nature (London) **377:**355–358.
21. **Jhappan, C., D. Gallahan, C. Stahle, E. Chu, G. H. Smith, G. Merlino, and R. Callahan.** 1992. Expression of an activated Notch-related int-3 transgene interferes with cell differentiation and induces neoplastic transformation in mammary and salivary glands. Genes Dev. **6:**345–355.
22. **Kopan, R., J. S. Nye, and H. Weintraub.** 1994. The intracellular portion of mouse Notch: a constitutively activated repressor of myogenesis directed at the basic helix-loop-helix region of MyoD. Development **120:**2385–2396.
23. **Kopan, R., and H. Weintraub.** 1993. Mouse notch: expression in hair follicles correlates with cell fate determination. J. Cell Biol. **121:**631–641.
24. **Kozak, M.** 1987. Effects of intercistronic length on the efficiency of reinitiation by eucaryotic ribosomes. Mol. Cell. Biol. **7:**3438–3445.
25. **Kozak, M.** 1989. The scanning model for translation: an update. J. Cell Biol. **108:**229–241.
26. **Lardelli, M., J. Dahlstrand, and U. Lendahl.** 1994. The novel Notch homologue mouse Notch 3 lacks specific epidermal growth factor-repeats and is

expressed in proliferating neuroepithelium. Mech. Dev. **46:**123–136.
27. **Lardelli, M., and U. Lendahl.** 1993. Motch A and motch B— —two mouse Notch homologues coexpressed in a wide variety of tissues. Exp. Cell Res. **204:**364–372.
28. **Larsson, C., M. Lardelli, I. White, and U. Lendahl.** 1994. The human NOTCH1, 2, and 3 genes are located at chromosome positions 9q34, 1p13-p11, and 19p13.2-p13.1 in regions of neoplasia-associated translocation. Genomics **24:**253–258.
29. **Levy, L. S., R. E. Fish, and G. B. Baskin.** 1988. Tumorigenic potential of a *myc*-containing strain of feline leukemia virus in vivo in domestic cats. J. Virol. **62:**4770–4773.
30. **Levy, L. S., M. B. Gardner, and J. W. Casey.** 1984. Isolation of a feline leukaemia provirus containing the oncogene myc from a feline lymphosarcoma. Nature (London) **308:**853–856.
31. **Levy, L. S., P. A. Lobelle-Rich, J. Overbaugh, J. L. Abkowitz, R. Fulton, and P. Roy-Burman.** 1993. Coincident involvement of *flvi*-2, c-*myc*, and novel *env* genes in natural and experimental lymphosarcomas induced by feline leukemia virus. Virology **196:**892–895.
32. **Lieber, T., S. Kidd, E. Alcamo, V. Corbin, and M. W. Young.** 1993. Antineurogenic phenotypes induced by truncated Notch proteins indicate a role in signal transduction and may point to a novel function for Notch in nuclei. Genes Dev. **7:**1949–1965.
33. **Linenberger, M. L., J. L. Rohn, S. Ellis-Smith, R. Ingber, and J. Overbaugh.** Submitted for publication.
34. **Maine, E. M., J. L. Lissemore, and W. T. Starmer.** 1995. A phylogenetic analysis of vertebrate and invertebrate Notch-related genes. Mol. Phylogenet. Evol. **4:**139–149.
35. **McDonough, S. K., S. Larsen, R. S. Brodey, N. D. Stock, and J. W. D. Hardy.** 1971. A transmissible feline fibrosarcoma of viral origin. Cancer Res **31:**953–956.
36. **Mount, S. M.** 1982. A catalogue of splice junction sequences. Nucleic Acids Res. **10:**459–472.
37. **Mullins, J. I., D. S. Brody, R. C. Binari, Jr., and S. M. Cotter.** 1984. Viral transduction of c-myc gene in naturally occurring feline leukaemias. Nature (London) **308:**856–858.
38. **Mullins, J. I., C. S. Chen, and E. A. Hoover.** 1986. Disease-specific and tissue-specific production of unintegrated feline leukaemia virus variant DNA in feline AIDS. Nature (London) **319:**333–336.
39. **Neil, J. C., D. Forrest, D. L. Doggett, and J. I. Mullins.** 1987. The role of feline leukaemia virus in naturally occurring leukaemias. Cancer Surv. **6:**117–137.
40. **Neil, J. C., R. Fulton, M. Rigby, and M. Stewart.** 1991. Feline leukemia virus: generation of pathogenic and oncogenic variants. Curr. Top. Microbiol. Immunol. **171:**67–93.
41. **Neil, J. C., D. Hughes, R. McFarlane, N. M. Wilkie, D. E. Onions, G. Lees, and O. Jarrett.** 1984. Transduction and rearrangement of the myc gene by feline leukaemia virus in naturally occurring T-cell leukaemias. Nature (London) **308:**814–820.
42. **Nye, J. S., R. Kopan, and R. Axel.** 1994. An activated Notch suppresses neurogenesis and myogenesis but not gliogenesis in mammalian cells. Development **120:**2421–2430.
43. **Onions, D., G. Lees, D. Forrest, and J. Neil.** 1987. Recombinant feline viruses containing the myc gene rapidly produce clonal tumours expressing T-cell antigen receptor gene transcripts. Int. J. Cancer **40:**40–45.
44. **Overbaugh, J., S. Dewhurst, and J. I. Mullins.** 1990. Proviral DNA cloning, p. 131–145. *In* A. Aldovini and B. D. Walker (ed.), Techniques in HIV research. Stockton Press, New York.
45. **Papenhausen, M. D., and J. Overbaugh.** 1993. Nucleotide sequence of the splice junction of feline leukemia virus envelope mRNA. Virology **195:**804–807.
46. **Reanume, A. G., R. A. Conlon, R. Zirngibl, T. P. Yamaguchi, and J. Rossant.** 1992. Expression analysis of a Notch homologue in the mouse embryo. Dev. Biol. **154:**377–387.
47. **Rebay, I., R. G. Fehon, and S. Artavanis-Tsakonas.** 1993. Specific truncations of Drosophila Notch define dominant activated and dominant negative forms of the receptor. Cell **74:**319–329.
48. **Robbins, J., B. J. Blondel, D. Gallahan, and R. Callahan.** 1992. Mouse mammary tumor gene *int-3*: a member of the *Notch* gene family transforms mammary epithelial cells. J. Virol. **66:**2594–2599.
49. **Rohn, J. L., M. L. Linenberger, E. A. Hoover, and J. Overbaugh.** 1994. Evolution of feline leukemia virus variant genomes with insertions, deletions, and defective envelope genes in infected cats with tumors. J. Virol. **68:**2458–2467.
50. **Sanger, F., S. Nicklen, and A. R. Coulson.** 1977. DNA sequencing with chain-terminating inhibitors. Proc. Natl. Acad. Sci. USA **74:**5463–5467.
51. **Snyder, S. P., and G. H. Theilen.** 1969. Transmissible feline fibrosarcoma. Nature (London) **221:**1074–1075.
52. **Stewart, M. A., D. Forrest, R. McFarlane, D. Onions, N. Wilkie, and J. C. Neil.** 1986. Conservation of the c-myc coding sequence in transduced feline v-myc genes. Virology **154:**121–134.
53. **Stifani, S., C. M. Blaumueller, N. J. Redhead, R. E. Hill, and S. Artavanis-Tsakonas.** 1992. Human homologs of a Drosophila Enhancer of split gene product define a novel family of nuclear proteins. Nat. Genet. **2:**119–127.
54. **Struhl, G., K. Fitzgerald, and I. Greenwald.** 1993. Intrinsic activity of the Lin-12 and Notch intracellular domains in vivo. Cell **74:**331–345.
55. **Swain, A., and J. M. Coffin.** 1992. Mechanism of transduction by retroviruses. Science **255:**841–845.
56. **Swiatek, P. J., C. E. Lindsell, F. F. del Amo, G. Weinmaster, and T. Gridley.** 1994. *Notch1* is essential for postimplantation development in mice. Genes Dev. **8:**707–719.
57. **Terry, A., R. Fulton, M. Stewart, D. E. Onions, and J. C. Neil.** 1992. Pathogenesis of feline leukemia virus T17: contrasting fates of helper, v-*myc*, and v-*tcr* proviruses in secondary tumors. J. Virol. **66:**3538–3549.
58. **Thomas, E., and J. Overbaugh.** 1993. Delayed cytopathicity of a feline leukemia virus variant is due to four mutations in the transmembrane protein gene. J. Virol. **67:**5724–5732.
59. **Tsatsanis, C., R. Fulton, K. Nishigaki, H. Tsujimoto, L. Levy, A. Terry, D. Spandidos, D. Onions, and J. C. Neil.** 1994. Genetic determinants of feline leukemia virus-induced lymphoid tumors: patterns of proviral insertion and gene rearrangement. J. Virol. **68:**8296–8303.
60. **Varmus, H. E.** 1990. Retroviruses and oncogenes I. Biosci. Rep. **10:**413–430.
61. **Weinmaster, G., V. J. Roberts, and G. Lemke.** 1991. A homolog of Drosophila Notch expressed during mammalian development. Development **113:**199–205.
62. **Weinmaster, G., V. J. Roberts, and G. Lemke.** 1992. *Notch2*: a second mammalian *Notch* gene. Development **116:**931–941.
63. **Zhang, J., and H. M. Temin.** 1993. 3′ junctions of oncogene-virus sequences and the mechanisms for formation of highly oncogenic retroviruses. J. Virol. **67:**1747–1751.
64. **Zhang, J., and H. M. Temin.** 1993. Rate and mechanism of nonhomologous recombination during a single cycle of retroviral replication. Science **259:**234–238.